Article

Discovery Medicine 2024; 36(183): 666–677
https://doi.org/10.24976/Discov.Med.202436183.63

Epithelial-Mesenchymal Transformation Promotes the Progression of Hepatocellular Carcinoma through NF-κB/MMP9 Axis

Jinsen Li[1], Qingbin Cai[2], Ziyue Wang[3], Liangshi Wang[2], Guangrun Yang[4], Zhilong Zhang[5], Na Ge[2], Shunxin Hu[3], Tian Bai[2,*]

[1]Nuclear Magnetic Resonance Department, Third Affiliated Hospital of Qiqihar Medical College, 161000 Qiqihar, Heilongjiang, China
[2]Radiographic Imaging Center, Third Affiliated Hospital of Qiqihar Medical College, 161000 Qiqihar, Heilongjiang, China
[3]Imaging Diagnosis, Qiqihar Medical College, 161006 Qiqihar, Heilongjiang, China
[4]Department of Radiotherapy, Third Affiliated Hospital of Qiqihar Medical College, 161000 Qiqihar, Heilongjiang, China
[5]Clinical Laboratory, Third Affiliated Hospital of Qiqihar Medical College, 161000 Qiqihar, Heilongjiang, China
*Correspondence: baitian8771145@qmu.edu.cn (Tian Bai)
Published: 20 April 2024

Background: Primary liver cancer (PHC) stands as one of the most prevalent malignant diseases in clinical settings. Studies have indicated that transcatheter arterial chemoembolization (TACE) treatment exhibits superior clinical outcomes, potentially increasing the complete necrosis rate in patients with PHC. A correlation exists between the clinical outcomes of TACE surgery and the process of epithelial-mesenchymal transition (EMT), yet the underlying mechanism remains a mystery. Hence, it is crucial to investigate the impact and mechanism of EMT on hepatocellular carcinoma (HCC).

Methods: Retrospectively, patients with advanced liver cancer who underwent TACE were selected and categorized into two groups based on the assessment of clinical efficacy: the effective group and the ineffective group. The expression levels of nuclear factor-kappa B (*NF-κB*), matrix metalloproteinase 9 (*MMP9*), *Ki-67*, B-cell lymphoma-2 (*Bcl-2*), Bcl-2-associated X (*Bax*), *Vimentin*, *E-cadherin*, and *N-cadherin* in tumor tissues were evaluated using reverse transcription-polymerase chain reaction (RT-PCR). *In vitro*, Huh7 cells were cultured, and lentivirus infections were utilized to inhibit the overexpression of NF-κB and MMP9. The determination of EMT and cell viability was conducted through Cell Counting Kit-8 (CCK-8) assays, RT-PCR, and Western blot.

Results: Sixty patients diagnosed with advanced liver cancer were selected for the study. Based on their clinical outcomes, 30 patients with advanced hepatocellular carcinoma were categorized into the effective group, while the remaining 30 patients were categorized into the ineffective group. The results of the Western blot analysis indicated that, in comparison to the effective group, the expression levels of NF-κB, MMP9, Ki-67, Bcl-2, Vimentin, and N-cadherin were significantly higher in the tumor tissues of the ineffective group. Conversely, the expression of Bax and E-cadherin was notably lower in the effective group. Following the individual knockdown of NF-κB and MMP9, the cell experiments revealed a remarkable decrease in the expression levels of Ki-67, Bcl-2, Vimentin, and N-cadherin, whereas the expression of Bax and E-cadherin showed significant elevation ($p < 0.05$). Furthermore, there was a significant increase in cell viability and a decrease in cell apoptosis after the knockdown of NF-κB and MMP9.

Conclusions: The NF-κB/MMP9 signaling axis serves as a pivotal regulator that fosters proliferation and impedes apoptosis in Huh7 cells by modulating the process of EMT.

Keywords: advanced hepatocellular carcinoma; EMT; MMP9; NF-κB

Introduction

Primary liver cancer (PHC) stands as one of the most prevalent malignant diseases observed in clinical settings, with hepatocellular carcinoma (HCC) representing the predominant pathological subtype [1]. The incidence of HCC is notably higher in China due to the widespread prevalence of hepatitis B virus infection compared to the international average. Epidemiological studies have underscored that in China, HCC ranks second only to lung cancer and gastric cancer in terms of incidence, posing a significant threat to patients' lives and health. Diagnosis for the majority of liver cancer patients typically occurs during the middle to late stages of the disease as early-stage liver cancer often presents with subtle symptoms [2,3].

Transcatheter arterial chemoembolization (TACE) is a commonly employed method in clinical practice for patients with inoperable HCC [4]. Studies have demonstrated the favorable clinical outcomes of TACE, resulting in an increased complete necrosis rate of up to 50.2% among pa-

tients with primary liver cancer [5]. Despite these promising results, a portion of patients fail to benefit from TACE. The objective remission rate (ORR) following TACE stands at 45%, indicating that 55% of patients do not experience relief despite undergoing this treatment [6]. Identifying the specific mechanisms responsible for the inefficacy of TACE in patients with primary liver cancer is essential to enhance the effectiveness of clinical treatment.

Studies have established a correlation between the clinical outcomes of TACE surgery and the phenomenon known as epithelial-mesenchymal transition (EMT) [7]. EMT plays a crucial role in tumor invasion and metastasis [8–10]. Moreover, extensive research has emphasized EMT as a primary regulator influencing the growth, invasion, and metastasis not only in liver cancer but also in prostate cancer and colon cancer [11–13]. Concurrently, numerous studies have highlighted a strong correlation between the therapeutic efficacy of TACE in patients with PHC and their levels of EMT. EMT has been identified to stimulate the proliferation, migration, and invasion of hepatocellular carcinoma cells, ultimately diminishing the clinical therapeutic efficacy of TACE [14]. However, consensus is lacking regarding the specific molecular mechanism governing the occurrence and progression of tumor cell EMT in PHC [15].

Matrix metalloproteinase 9 (MMP9), by degrading the extracellular matrix, plays a role in accelerating tumor invasion and EMT [16]. Both nuclear factor-kappa B (NF-κB) and MMP9 have been associated with EMT in malignant tumor tissues [17]. A previous study has affirmed NF-κB as an upstream regulator of MMP9, and the NF-κB/MMP9 signaling axis as a principal factor contributing to the onset and progression of chronic inflammatory diseases [18]. Nonetheless, there remains uncertainty about whether NF-κB and MMP9 mutually regulate each other in PHC tumors and the specific regulatory mechanisms governing EMT.

This study hypothesized that the NF-κB/MMP9 signaling axis within hepatocellular carcinoma cells might effectively enhance tumor cell proliferation, elevate EMT levels, suppress cell apoptosis, and consequently facilitate the onset and progression of tumors.

Materials and Methods

Reagents

Dulbeccos modified eagle medium (DMEM) (No.12800017, Gibco BRL, Grand Island, NY, USA,), Fetal Bovine Serum (Hyclone Company, Logan, UT, USA, Catalog No.: SH30396.03), and phosphate buffer solution (PBS) supplemented with penicillin-streptomycin (Hyclone, Logan, UT, USA, Catalog No.: SH30256.01) were utilized for cell cultivation. Cell viability was assessed primarily using the Cell Counting Kit-8 (CCK-8) (Solebo Technology Co., Ltd., Shanghai, China, Catalog No.: CA1210).

For the reverse transcription-polymerase chain reaction (RT-PCR) technique, a reverse transcription kit (Takara Company, Liaoning, China, Catalog No.: RR047A) and qPCR Kit (Takara Company, Liaoning, China, Catalog No.: RR430B) were employed. In the Western blot analysis to determine protein expression, Anti-E-Cadherin (Abcam, Cambridge, UK, Catalog No.: ab40772, 1:2000 dilution), Anti-N-Cadherin (Abcam, Cambridge, UK, Catalog No.: ab76011, 1:2000 dilution), Anti-Vimentin (Abcam, Cambridge, UK, Catalog No.: ab92547, 1:2000 dilution), and Anti-glyceraldehyde-3-phosphate dehydrogenase (GAPDH) (Abcam, Cambridge, UK, Catalog No.: ab8245, 1:2000 dilution) antibodies were utilized. Secondary antibodies included goat anti-rabbit IgG H&L (horseradish peroxidase, HRP) (Abcam, Cambridge, UK, Catalog No.: ab205718) and goat anti-mouse IgG H&L (HRP) (Abcam, Cambridge, UK, Catalog No.: ab205719).

Clinical Researches

Patients Selection and Sample Collection

Retrospectively, we collected primary liver cancer (PHC) patients who underwent TACE treatment at our hospital. Inclusion criteria for PHC patients were as follows: (1) Patients meeting the diagnostic and treatment criteria for PHC [19]; (2) Confirmed diagnosis via histopathology and imaging; (3) Karnofsky functional status score (KPS) $\geq$60; (4) Tumor-Node-Metastasis (TNM) stage IIa to IIIb; (5) No contraindications for TACE operation; (6) Informed consent obtained from all patients; (7) Complete clinical and imaging data available before and after the operation.

The exclusion criteria for PHC patients were as follows: (1) Estimated survival time of less than 6 months; (2) Presence of immunosuppression; (3) Coagulation dysfunction or active gastrointestinal bleeding; (4) Hepatic and renal insufficiency; (5) Previous history of targeted drug therapy or radiotherapy; (6) Presence of malignant tumors in other body parts.

TACE Operation

Patients diagnosed with PHC underwent TACE treatment post-admission. The chemotherapy regimen involved GEMOX, comprising gemcitabine administered at a dosage of 800 mg to 1000 mg per square meter (m^2) and oxaliplatin at a dosage of 85–100 mg/m^2. The procedure involved hepatic artery embolization with the concurrent injection of chemotherapeutic agents. Injections were administered monthly and repeated thrice. Subsequently, tumor tissue was obtained via hepatocyte puncture after the third injection and stored for subsequent detection.

Efficacy Evaluation

Abdominal magnetic resonance imaging (MRI) (Tangshan Ruijian Technology Co., Ltd., Tangshan, China) examinations were conducted both before and after the treatment. The therapeutic efficacy was evaluated based on

Table 1. Primer sequence of each mRNA.

mRNA	Sequence
NF-κB	F 5′CCTTCCTCATCCCATCTTTGAC3′
	R 5′ACCTCAATGTCCTCTTTCTGC3′
MMP9	F 5′GCCACTACTGTGCCTTTGAGTC3′
	R 5′CCCTCAGAGAATCGCCAGTACT3′
Ki-67	F 5′GTAGAAGAGGAACCCAGCAGGAGA3′
	R 5′GCTTTGCCAGCAGTCAGTGATTC3′
Bax	F 5′AGAGGGCCCATCACTGAGAA3′
	R 5′CTCCGCCCCATAGTTACCTG3′
Bcl-2	F 5′ATAGCTGTTGCCCACTCGAC3′
	R 5′ATCTATGCCCAACAGGCCAC3′
E-cadherin	F 5′CCAGCTACTAGAGAGGCTG3′
	R 5′CACAGGTGCTTTGCAGTTCC3′
N-cadherin	F 5′TGAAGTCCCCAATGTCTCCA3′
	R 5′GCATCATCATCCTGCTTATCC3′
Vimentin	F 5′TCAGACAGGATGTTGACAAT3′
	R 5′GACATGCTGTTCCTGAATCT3′
GAPDH	F 5′GAACGGGAAGCTCACTGG3′
	R 5′GCCTGCTTCACCACCTTCT3′
MMP-9-ov	F 5′GGACTCGGTCTTTGAGGAGC3′
	R 5′AGCCAGTTTGCCGGATACAAACTGGTATTC3′
si-MMP-9	F 5′ACCCTGGGGAAGGAGCCAGTTTGGCCGAA AGUUUCACCAATACTGTTCTGGAGGAAA3′
	R 5′TTTCCTCCAGAACAGTATTGGTGUUUCTTT CGGCCAAACTGGCTCCTTC3′
si-NF-κB	F 5′CACTGTAACTGCTGGACCCAAGG3′
	R 5′CGCCTCTGTCATTCGTGCTTCC3′
NF-κB-ov	F 5′GACTAGACGGAAGCACGCACAAG3′
	R 5′GCACGCAGTAGGGATACACACAG3′

NF-κB, nuclear factor-kappa B; *MMP9*, matrix metalloproteinase 9; *Bax*, Bcl-2-associated X; *Bcl-2*, B-cell lymphoma-2; *GAPDH*, glyceraldehyde-3-phosphate dehydrogenase.

the criteria outlined in the Efficacy Evaluation Criteria of Solid Tumors Version 1.1 (RECIST Version 1.1, National Cancer Institute of USA) [19]. The evaluation involved grading according to changes observed in the size of target lesions before and after the treatment. Therapeutic effectiveness was categorized as follows: Complete Remission (CR), denoting the disappearance of target lesions and a reduction of the short diameter of all pathological lymph nodes (including both target and non-target nodules) to 10 mm or less; Partial Remission (PR), indicated by a minimum of 30% reduction in the total diameter of target lesions compared to the baseline level. Disease Progression (PD) is identified when there's a 20% increase in the diameter of target lesions compared to the smallest sum measured throughout the study, with an absolute increase of at least 5 mm. The presence of new lesions also qualifies as disease progression. Disease Stability (SD) is characterized by a reduction in target lesions that doesn't meet the criteria for PR or an increase that doesn't meet the criteria for PD. As per the efficacy criteria of TACE, patients with PHC were categorized into two groups: the CR PR group (indicating effective treatment) and the SD PD group (representing ineffective treatment).

Cell Culture

The human hepatoma epithelial cell line HuH7 (obtained from the Shanghai Cell Bank of the Chinese Academy of Sciences, Shanghai, China, Catalog No.: CTCC-003-0019) [19] was inoculated into 6-well plates and maintained at 37 °C in a 5% CO_2 cell incubator. The DMEM medium was replenished every 24 h. Short tandem repeat (STR) validation and mycoplasma testing were conducted and validated.

Real-Time PCR

Total cellular RNA was extracted using the Trizol reagent (R0016, Beyotime Biotechnology, Shanghai, China). A total of 2 µg RNA was utilized for cDNA synthesis in a 20-µL reaction using a Reverse Transcription Kit. Equal amounts of resulting cDNA were used for PCR under the following conditions: initial denaturation at 95 °C for 10 min, followed by 40 cycles of 95 °C for 15 s and 60 °C for 1 min, and a final extension step at 72 °C for 5 min. Each sample was analyzed in triplicate, and the $2^{-\Delta\Delta CT}$ method was employed for quantitative assessment, with GAPDH serving as the internal control. Real-time PCR primer sequences are detailed in supporting Table 1. GraphPad Prism v7 (GraphPad Software, San Diego, CA, USA) was used to generate histograms.

Lentivirus Infection

Overexpressed Lentivirus Infection

The NF-κB-ov and MMP9-ov overexpression Lentivirus vectors were developed by Shanghai Jima Biology Co., Ltd. (Shanghai, China). Pre-test results indicated an infection efficacy of 2×10^7 TU/mL (MOI = 20) for NF-κB-ov and 1×10^7 TU/mL (MOI = 10) for MMP9-ov. Huh7 cell lines were seeded at a density of 2×10^5 cells/mL in 24-well plates and cultured in a constant temperature cell incubator. Subsequently, the culture medium was replaced according to the transfection system, and the respective lentivirus was introduced for cell infection, following which the cells were incubated at 37 °C. The cellular status was assessed after 8–12 h, and fresh medium was substituted. The infection efficiency was evaluated using the qRT-PCR technique.

siRNA Silencing Transfection

Lipofectamine™ 2000 (Invitrogen, Carlsbad, CA, USA) was employed for transfecting small interfering RNA (siRNA). siNF-κB and siMMP9 were developed by Shanghai Jima Biology Co., Ltd. (Shanghai, China). A total of 5×10^5 Huh-7 cells were transfected with 20 nM siRNA using LTX reagent (Invitrogen Carlsbad, CA, USA) accord-

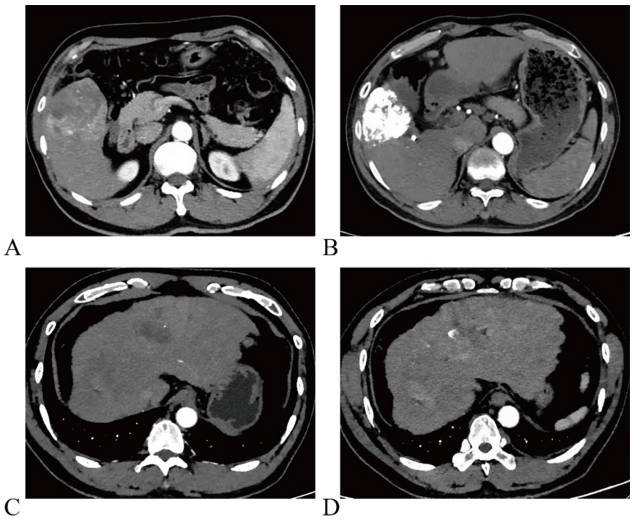

Fig. 1. The efficacy evaluation by MRI imaging based on comparisons between before and after treatment. (A) The effective response before treatment (n = 30). (B) The effective response after treatment (n = 30). (C) The ineffective response before treatment (n = 30). (D) The ineffective response after treatment (n = 30). MRI, magnetic resonance imaging.

ing to the manufacturer's protocol. After 12 h, the culture medium was replaced, and subsequent experiments were conducted after 24 or 48 h.

Cell Counting Kit-8 (CCK-8)

Cells were plated onto 96-well plates and cultured for 0, 1, 2, 3, 4, and 5 days, respectively. The absorbance was measured using the BioTek 800 TS Enzyme Labeler (800 TS, Agilent BioTek, Norgen, NU). The absorbance at 450 nm of the Cell Counting Kit-8 (CCK-8) solution (Solebo Technology Co., Ltd., Shanghai, China, item No.: CA1210) was assessed to calculate the cell growth rate.

Western Blot

The cells were lysed using radioimmunoprecipitation assay (RIPA) buffer (iNtRON Biotechnology, Seoul, Korea), supplemented with phosphatase and protease inhibitor cocktail (Thermo Scientific, Rockford, IL, USA). The Pierce™ BCA assay (Thermo Fisher Scientific, Rockford, IL, USA) was utilized to quantify protein concentrations. Subsequently, equal amounts of protein (10 µg) from each sample were subjected to electrophoresis on 8–15% SDS-polyacrylamide gels. The separated proteins were transferred onto a polyvinylidene difluoride (PVDF) membrane (ATTO Co., Ltd., Tokyo, Japan). Following this, the membrane was incubated with primary antibodies, followed by incubation with a conjugated secondary antibody tagged with peroxidase.

The obtained proteins were detected using the electrochemiluminescence (ECL) detection system (Bio-Rad Laboratory, Hercules, CA, USA), and subsequently analyzed with the Image Lab 4.1 software (Bio-Rad Laboratory, Hercules, CA, USA). The densitometry readings of the protein bands were normalized by comparing them with the expression of GAPDH as a control, utilizing the ImageJ software program (U.S. National Institutes of Health, Bethesda, MD, USA).

Table 2. Demographic, clinical profile of study population and comparison between CR+PR group and SD+PD group.

Parameters	CR+PR group (n = 30)	SD+PD group (n = 30)	t.val/x^2	*p*.val
Age, years	56.43 ± 6.59	55.83 ± 7.65	0.325	0.746
Male (%)	17 (56.7%)	20 (66.7%)	0.635	0.426
Tumor size (cm)	4.31 ± 1.23	5.23 ± 0.87	–3.330	0.002
ECOG	1.73 ± 0.58	1.10 ± 0.31	5.27	<0.001
KPS	72.83 ± 6.42	64.83 ± 5.56	5.159	<0.001
TNM stage			0.410	0.938
IIa	10	8		
IIb	6	7		
IIIa	10	10		
IIIb	4	5		

CR, Complete Remission; PR, Partial Remission; SD, Disease Stability; KPS, Karnofsky functional status score; ECOG, Eastern Cooperative Oncology Group; TNM, Tumor-Node-Metastasis; PD, Disease Progression.

Statistical Analysis

Statistical analysis for this study was conducted using SPSS version 26.0 software (SPSS Inc., Chicago, IL, USA). Data were presented as means ± standard deviation (SD). A Student *t*-test was performed for comparisons between two groups, while comparisons involving three or more groups were analyzed using one-way Analysis of Variance (ANOVA) followed by the Tukey-Kramer Honestly Significant Difference (HSD) test. Chi-square analysis and Student *t*-test were utilized for comparisons between two groups. A significance level of $p < 0.05$ was considered statistically significant.

Results

Comparative Analysis of Basic Clinical Information before Treatment between the Two Groups

A total of 60 patients diagnosed with advanced PHC and treated with TACE were included in this study. Fig. 1A,B illustrated the MRI characteristics of patients who exhibited effective treatment, while Fig. 1C,D demonstrated the MRI features of patients with ineffective treatment. These patients were divided into two groups based on the assessment of clinical efficacy: the effective group (30 patients) and the ineffective group (30 patients). Table 2 presented the comparison between these two groups. There were no statistically significant differences observed in age,

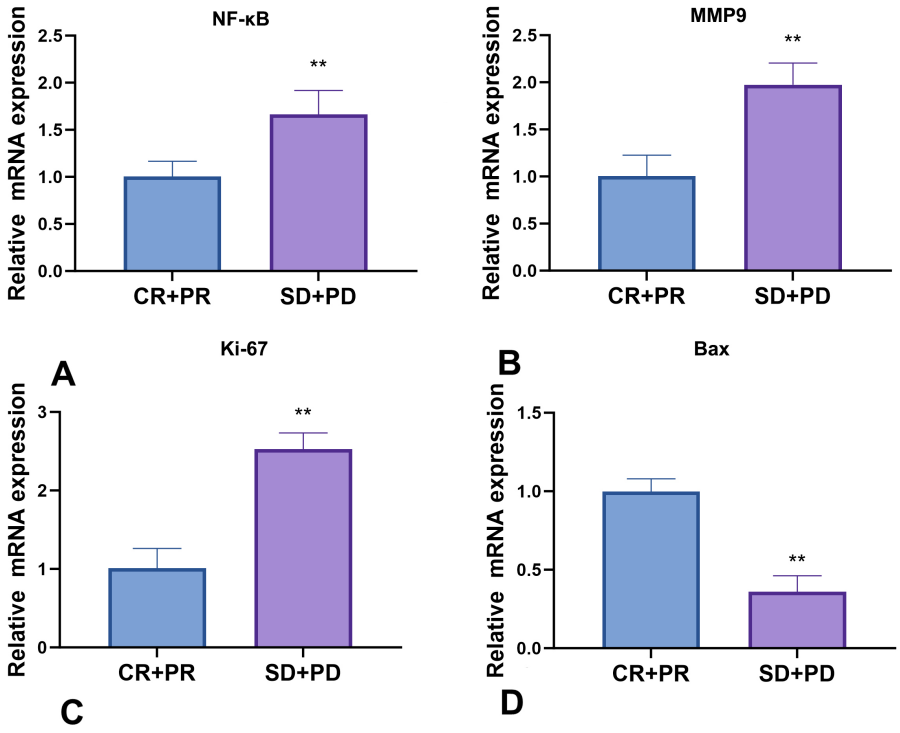

Fig. 2. The mRNA expression detection between groups. (A) The expression of NF-κB in CR+PR group and SD+PD group. (B) The expression of MMP9 in CR+PR group and SD+PD group. (C) The expression of Ki-67 in CR+PR group and SD+PD group. (D) The expression of Bax in CR+PR group and SD+PD group. **$p < 0.01$.

gender, or TNM stage between the two groups ($p > 0.05$). The tumor size in effective group was significantly smaller than that in ineffective group, and the Eastern Cooperative Oncology Group (ECOG) score and KPS score in effective group were significantly higher ($p < 0.05$).

Comparative Analysis of Gene Expression Detected by RT-PCR

RT-PCR analysis indicated significantly elevated levels of *NF-κB* and *MMP*-related mRNA expression in tumor tissue from the ineffective group compared to the effective group ($p < 0.01$, Fig. 2A,B). Furthermore, the expression of the proliferation-related gene *Ki-67* was markedly higher in the ineffective group than in the effective group ($p < 0.01$, Fig. 2C). Conversely, the expression of the apoptosis-related gene Bcl-2-associated X (*Bax*) was significantly lower in the ineffective group compared to the effective group ($p < 0.01$, Fig. 2D).

The expression of B-cell lymphoma-2 (*Bcl-2*) was notably higher in the ineffective group compared to the effective group ($p < 0.01$, Fig. 3A). Moreover, the expression levels of Vimentin and N-cadherin, both associated with EMT, were significantly elevated in the ineffective group in contrast to the effective group ($p < 0.01$, Fig. 3B,C). Additionally, the expression of E-cadherin was markedly lower in the ineffective group compared to the effective group ($p < 0.01$, Fig. 3D).

The observed trends highlight a significant upregulation of proliferation-related genes, a notable decrease in apoptosis-related genes, and a substantial elevation in EMT-related gene expression levels within liver cancer tissues of the ineffective group compared to the effective group. Concurrently, there was a considerable increase in the expression of NF-κB and MMP-related mRNA. These findings strongly suggest a plausible correlation between NF-κB, MMP, and EMT in hepatocellular carcinoma cells.

Effects of Knocking Down NF-κB and MMP9 on Proliferation, Apoptosis and EMT of Hepatoma Cells

The CCK-8 test demonstrated a notable decrease in Huh7 cell viability subsequent to NF-κB and MMP9 knockdown ($p < 0.05$, Fig. 4A). RT-PCR results revealed a significant reduction in the expression of NF-κB and MMP9 in Huh7 cells following NF-κB knockdown ($p < 0.05$, Fig. 4B,C). Additionally, the assessment of proliferation-related gene Ki-67 and apoptosis-related gene Bax expression via RT-PCR indicated a marked decrease in Ki-67 expression ($p < 0.05$, Fig. 4D,E).

Following the knockdown of NF-κB and MMP9 genes, EMT-related protein expressions in Huh7 cells were assessed via Western blot analysis. The results exhibited significantly reduced levels of Vimentin and N-cadherin expressions compared to the control group, while E-cadherin expression notably increased ($p < 0.05$, Fig. 5). These find-

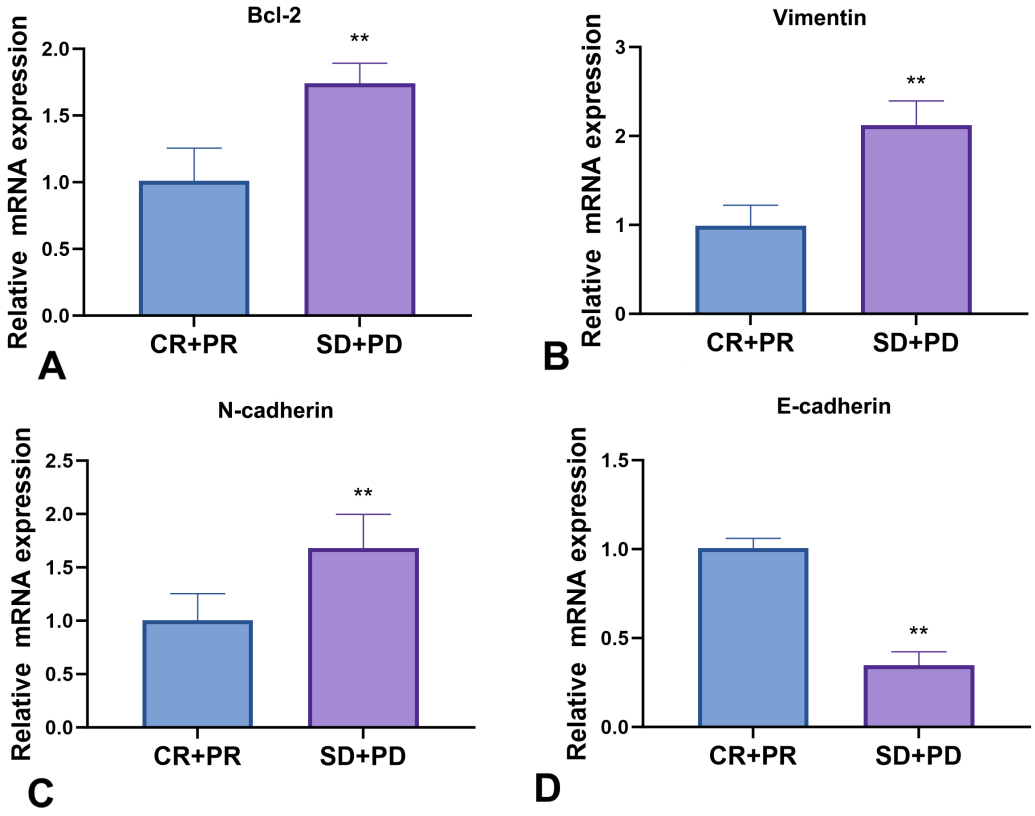

Fig. 3. The mRNA expression detection of Bcl-2 and EMT correlated genes between groups. (A) The expression of Bcl-2 in CR+PR group and SD+PD group. (B) The expression of Vimentin in CR+PR group and SD+PD group. (C) The expression of N-cadherin in CR+PR group and SD+PD group. (D) The expression of E-cadherin in CR+PR group and SD+PD group. $^{**}p < 0.01$. CR+PR: effective group; SD+PD: ineffective group. EMT, epithelial-mesenchymal transition.

ings indicate that upon NF-κB and MMP9 knockdown, the proliferation rate of Huh7 cells decreased, apoptosis levels increased, and the extent of EMT was notably diminished.

Effect of NF-κB/MMP9 Signal Axis on Proliferation, Apoptosis and EMT of Hepatoma Cells

The CCK-8 assay revealed that the combination of NF-κB knockdown and MMP9 overexpression did not significantly alter cell activity. However, when NF-κB was overexpressed alongside MMP9 knockdown, a notable decrease in cell viability was observed ($p < 0.05$, Fig. 6A). Additionally, the mRNA expression of NF-κB exhibited a significant decrease upon NF-κB knockdown in combination with MMP9 overexpression, whereas its expression increased upon NF-κB and MMP9 overexpression ($p < 0.05$, Fig. 6B).

The expression of MMP9 mRNA notably increased upon NF-κB knockdown combined with MMP9 overexpression, whereas it significantly decreased upon NF-κB overexpression in conjunction with MMP9 knockdown ($p < 0.05$, Fig. 6C). Ki-67 and the apoptosis-related gene Bax expression were evaluated using RT-PCR. The findings indicate no significant difference in Ki-67 expression compared to the control group. However, upon overexpression of NF-κB accompanied by MMP9 knockdown, Ki-67 expression in Huh7 cells markedly decreased ($p < 0.05$, Fig. 6D).

After knocking down NF-κB and overexpressing MMP9, Bax expression did not significantly differ from the control group. However, a sharp decline in Bax expression was observed in Huh7 cells following the overexpression of both NF-κB and MMP9 ($p < 0.05$, Fig. 6E). The Western blot results revealed no significant difference in the expression levels of EMT-related proteins Vimentin and N-cadherin between the NF-κB knockdown combined with MMP9 overexpression group and the control group. However, there was a significant decrease in the expression of Vimentin and N-cadherin in Huh7 cells when NF-κB was overexpressed alongside MMP9 knockdown ($p < 0.05$, Fig. 7).

Discussion

Combining clinical sample analysis with fundamental cell experiments, this research elucidated the effective role of the NF-κB signaling axis in promoting liver cancer proliferation. The occurrence and progression of EMT

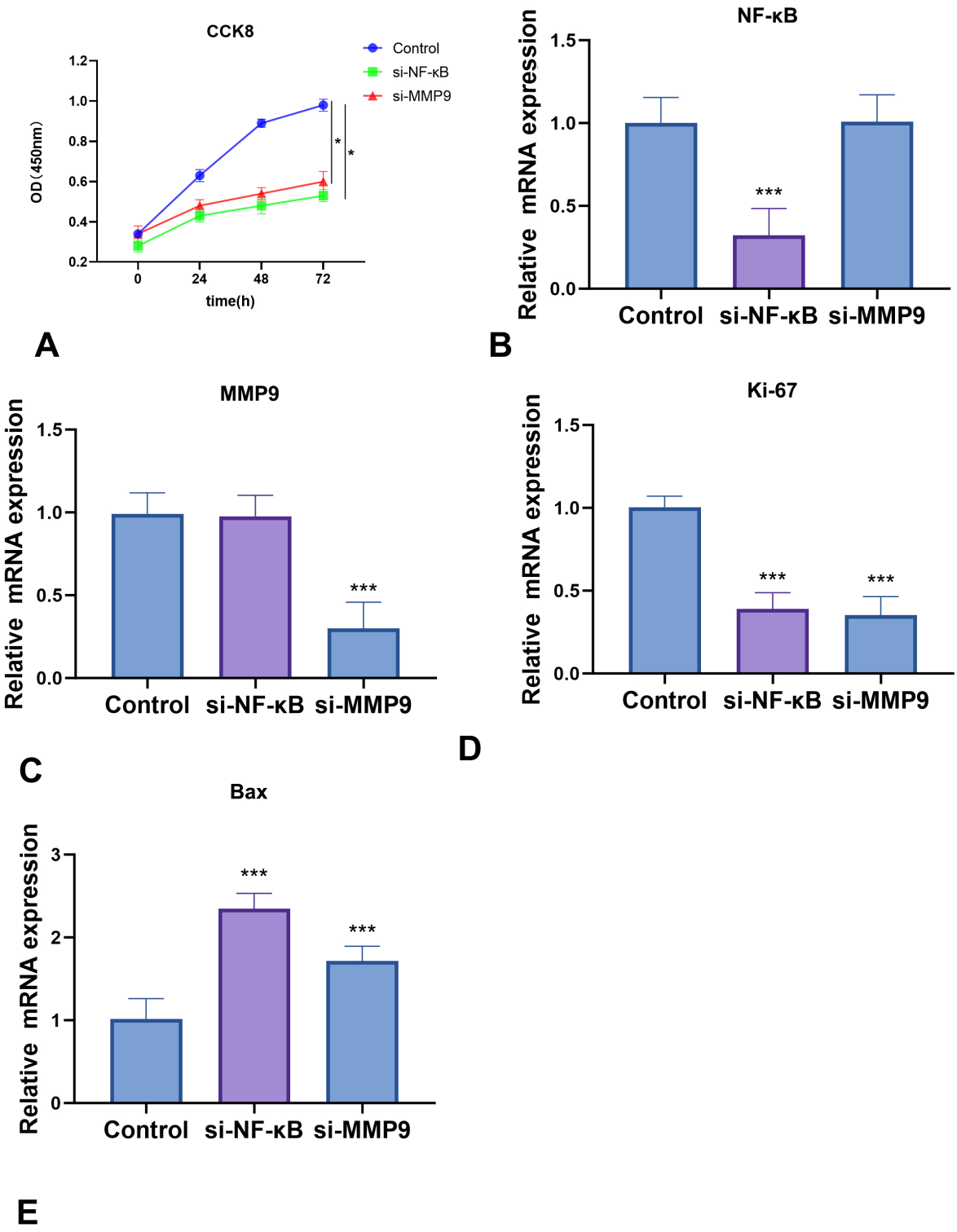

Fig. 4. Effects of NF-κB and MMP9 on the proliferation and apoptosis ability of Huh7 cells. (A) CCK-8 test to determine the cell proliferation ability with si-NF-κB or si-MMP9 infection. (B,C) RT-PCR to detect the NF-κB and MMP9 expression with si-NF-κB or si-MMP9 infection. (D) RT-PCR technique to determine the Ki-67 expression in Huh7 cells with si-NF-κB or si-MMP9 infection. (E) RT-PCR technique to determine the Bax expression in Huh7 cells with si-NF-κB or si-MMP9 infection. *$p < 0.05$ vs control; ***$p < 0.001$ vs Control. CCK-8, Cell Counting Kit-8; RT-PCR, reverse transcription-polymerase chain reaction.

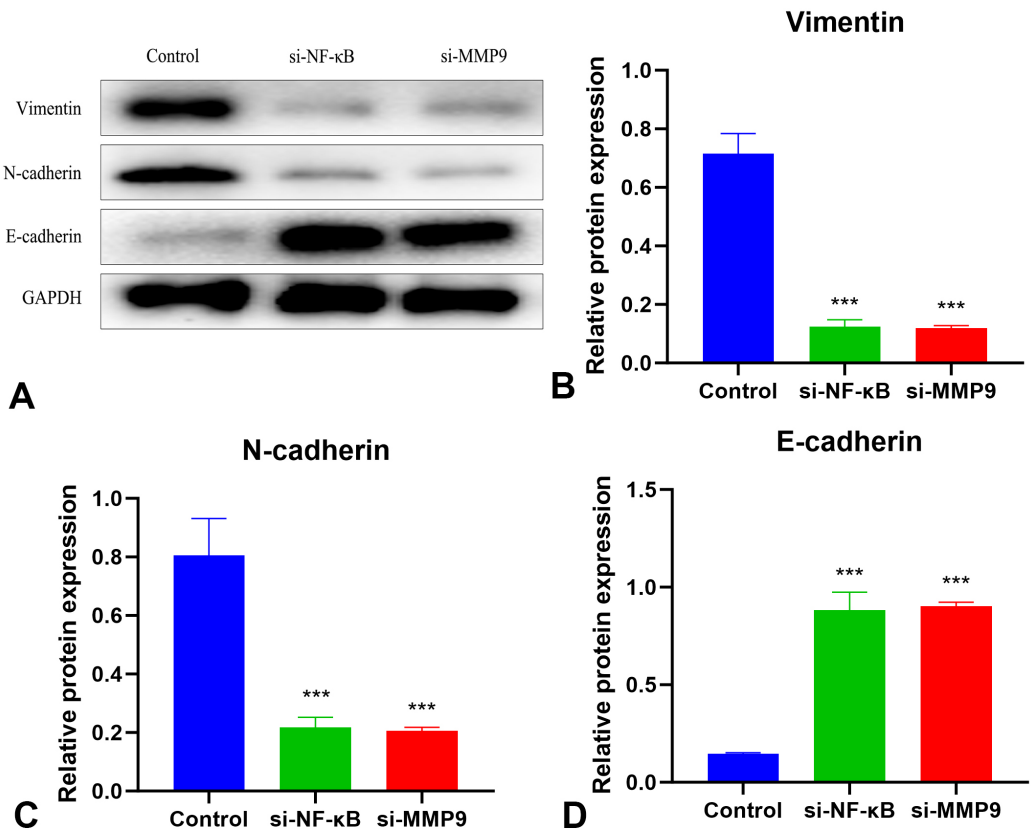

Fig. 5. Effects of NF-κB and MMP9 on the EMT of Huh7 cells. (A) Western blot experiments to determine the EMT correlated proteins expression. The expression of Vimentin (B), N-cadherin (C) and E-cadherin (D) in Huh7 cells with si-NF-κB or si-MMP9 infection. ***$p < 0.001$ vs Control.

significantly correlate with the invasiveness of hepatocellular carcinoma. EMT refers primarily to the morphological transition of epithelial cells, altering from a compact, cobblestone-like state to an elongated, fibrous cell-like state. This transformation results in the loss of cell polarity, weakened cell adhesion, increased motility, disrupts cell-cell junctions, facilitates cell movement and migration, thereby augmenting the invasiveness and metastatic potential of tumor cells [20–22].

The presence of EMT in liver cancer correlates with the tumor's invasive potential. A survival analysis conducted on liver cancer patients revealed a direct relationship between elevated EMT levels and diminished survival times, poorer therapeutic outcomes, and bleaker prognoses [23,24]. This study assessed the expression of EMT-related proteins in tumor tissues from two distinct patient groups based on the effectiveness of liver cancer treatments. The findings indicated notably higher levels of N-cadherin and Vimentin expression in tumor tissues of patients who experienced ineffective treatment compared to those in the group with effective treatment.

Hence, this study posits a strong association between the level of EMT in liver cancer cells and the clinical therapeutic outcomes observed in patients with this condition. Significantly elevated levels of NF-κB and MMP9 expression were noted in tumor tissues of the ineffective treatment group in contrast to the effective treatment group. Consequently, these findings underscore the potential significance of NF-κB and MMP9 in regulating EMT within hepatocellular carcinoma cells.

NF-κB, recognized as a conventional signaling molecule, plays pivotal roles in cell proliferation, apoptosis, immunological responses, and stress management [25]. Research has demonstrated that NF-κB activation contributes to the upregulation of chemokines, inflammatory proteins, and anti-apoptotic factors (such as Bcl-2), thereby fostering tumor cell proliferation, enhancing migration, and impeding apoptosis [26]. Moreover, studies have indicated that NF-κB activation elevates the expression of chemokines, inflammatory factors, and anti-apoptosis factors (specifically Bcl-2), promoting tumor cell proliferation and migration while inhibiting apoptosis occurrence [27]. Furthermore, NF-κB exhibits a distinct influence on tumor tissue's EMT [28]. Upon activation, NF-κB has been observed to stimulate Vimentin production in cells, thereby facilitating the onset of EMT [29].

MMP9, the matrix metalloproteinase (MMP) with the largest molecular weight among its family of protein

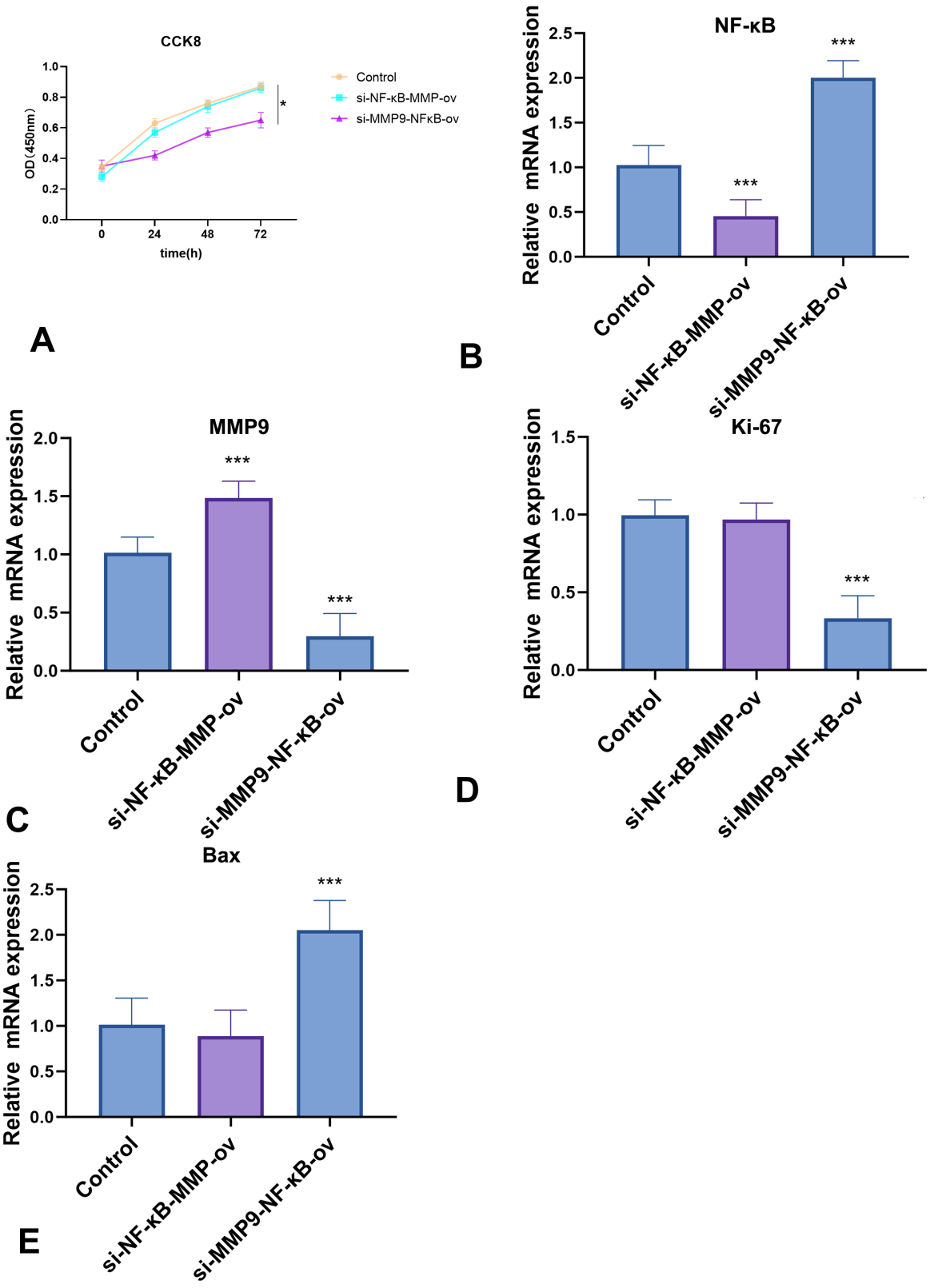

Fig. 6. Effects of NF-κB/MMP9 axis on the proliferation and apoptosis ability of Huh7 cells. (A) CCK-8 test to determine the cell proliferation ability with NF-κB/MMP9 axis blocked. (B,C) RT-PCR to detect the NF-κB and MMP9 expression with NF-κB/MMP9 axis blocked. (D) RT-PCR technique to determine the Ki-67 expression in Huh7 cells with NF-κB/MMP9 axis blocked. (E) RT-PCR technique to determine the Bax expression in Huh7 cells with NF-κB/MMP9 axis blocked. *$p < 0.05$ vs control; ***$p < 0.001$ vs Control.

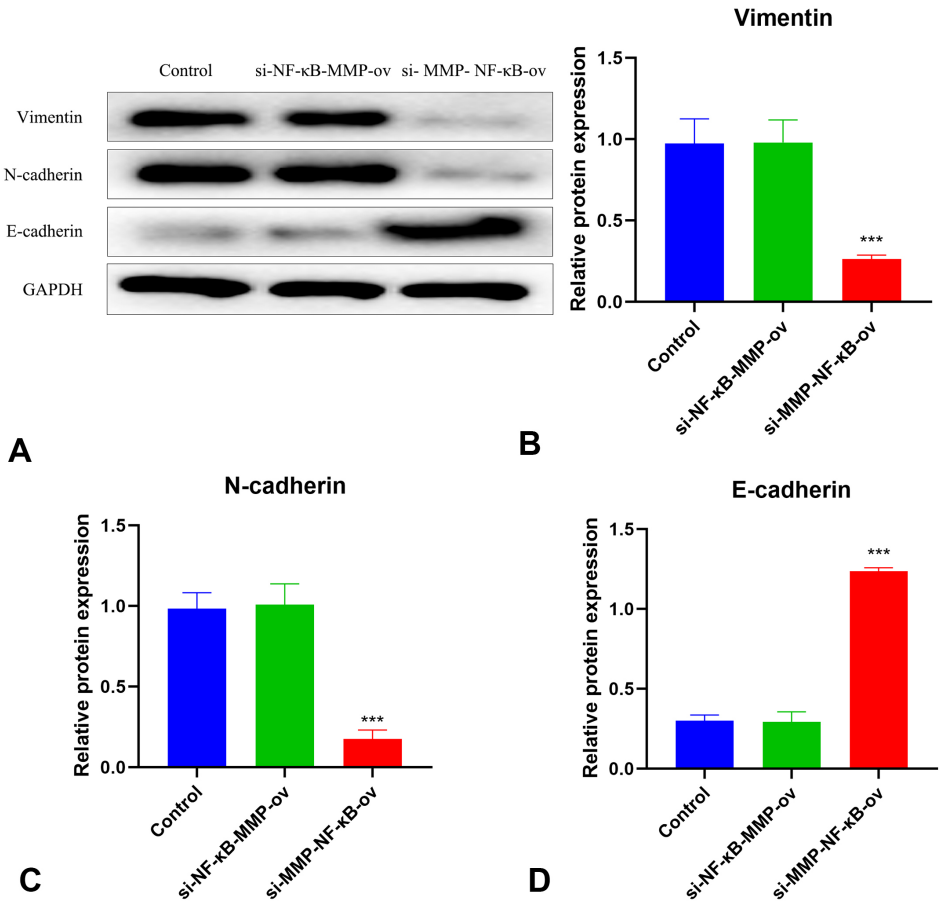

Fig. 7. Effects of NF-κB/MMP9 axis on the EMT of Huh7 cells. Western blot experiments to determine the EMT correlated proteins expression (A). The expression of Vimentin (B), N-cadherin (C) and E-cadherin (D) in Huh7 cells with NF-κB/MMP9 axis blocked. ***$p < 0.001$ vs Control.

molecules, plays a pivotal role in type IV collagen degradation [30]. Its activity induces extracellular matrix (ECM) breakdown and remodeling *in vivo*. Studies have specifically highlighted increased MMP9 expression in various tumor illnesses such as esophageal cancer, cervical cancer, and rectal cancer, correlating closely with tumor cell migration and invasion [31]. On one hand, MMP9 functions by degrading the extracellular matrix, leading to an accumulation of growth-promoting factors around cancer cells. This action aims to hinder apoptosis and promote the proliferation of tumor cells.

On the other hand, MMP9 exhibits a close association with tumor invasion, metastasis, and angiogenesis [32]. Simultaneously, MMP9 plays a significant role in promoting the occurrence of EMT within tumor cells [33]. To assess the impact of NF-κB and MMP9 on hepatocellular carcinoma, cell experiments were conducted using the Huh7 cell line, employing lentivirus infection techniques to suppress NF-κB and MMP9 expression. The findings reveal a notable decrease in Huh7 cell proliferation, a significant increase in apoptosis, and a marked reduction in EMT levels upon the suppression of NF-κB and MMP9. This study provides evidence that NF-κB and MMP9 actively promote hepatocellular carcinoma cell proliferation, hinder apoptosis, and contribute to the initiation and progression of EMT.

Research indicates a reciprocal regulatory relationship between NF-κB and MMP9. NF-κB can directly augment MMP9 expression by binding to its promoter region, as observed in various studies [34]. Strong associations have been unveiled between the NF-κB/MMP9 signaling axis and the emergence and progression of chronic inflammatory disorders like atherosclerosis and endometriosis [35]. Concurrently, investigations have highlighted the close correlation between heightened NF-κB and MMP9 expression and tumor invasiveness [36]. Nevertheless, whether NF-κB and MMP9 interact in the regulation of tumor EMT remains unknown, and no pertinent research reports currently exist. In this study, alterations in cellular functionality were observed by simultaneously knocking down MMP9 and overexpressing NF-κB. The results demonstrated a significant reduction in EMT, an increase in apoptosis, and a significant inhibition of cellular activity.

Conversely, when examining the cellular responses subsequent to NF-κB knockdown in conjunction with

MMP9 overexpression, no significant alterations in cell proliferation, apoptosis, or EMT levels were observed. The findings demonstrate that with suppressed cell activity, increased apoptosis, and reduced EMT levels, the combined effect of NF-κB knockdown and MMP9 overexpression yielded no substantial changes in cell functionality regarding proliferation, apoptosis, or EMT levels. Therefore, this study suggests that within hepatocellular carcinoma cells, NF-κB facilitates cell proliferation, inhibits apoptosis, and fosters EMT transformation by upregulating the expression of MMP9.

However, there are notable limitations in this study. The exploration of the NF-κB/MMP9 signaling axis and its impact on Huh7 cell function, activity, and EMT was conducted *in vitro*, which may not entirely replicate the complex *in vivo* conditions.

Conclusions

Throughout the treatment of advanced liver cancer patients, elevated EMT levels correlate with increased cell proliferation and reduced apoptosis, resulting in poorer therapeutic outcomes. Moreover, tumor tissues from patients with ineffective treatment display significantly heightened expression of NF-κB and MMP9. The upregulation of NF-κB/MMP9 actively fosters Huh7 cell proliferation, impedes apoptosis, and facilitates the onset and progression of EMT, ultimately contributing to tumor progression.

Availability of Data and Materials

The data used to support the findings of this study are included within the article.

Author Contributions

Conceptualization and design: TB. Data collection and curation: JL, NG, LW. Data analysis and interpretation: QC, ZZ, GY, ZW, SH. Manuscript writing: All authors. Final approval of manuscript: All authors. Agreed to be accountable for all aspects of the work in ensuring that questions related to the accuracy or integrity of any part of the work are appropriately investigated and resolved: All authors.

Ethics Approval and Consent to Participate

All subjects and their guardians provided informed consent, and the study protocols were exempted by the Ethics Committee of the Third Affiliated Hospital of Qiqihar Medical University (Approval No.: 2022LL-113).

Acknowledgment

Not applicable.

Funding

This research was funded by Innovation and Incentive Scheme of Qiqihar Science and Technology Program, grant No. CSFGG-2022181.

Conflict of Interest

The authors declare no conflict of interest.

References

[1] Jiang J, Dong W, Zhang W, Wang Q, Wang R, Wang J, *et al*. LncRNA SLC1A5-AS/MZF1/ASCT2 Axis Contributes to Malignant Progression of Hepatocellular Carcinoma. Discovery Medicine. 2023; 35: 995–1014.

[2] Konyn P, Ahmed A, Kim D. Current epidemiology in hepatocellular carcinoma. Expert Review of Gastroenterology & Hepatology. 2021; 15: 1295–1307.

[3] Samant H, Amiri HS, Zibari GB. Addressing the worldwide hepatocellular carcinoma: epidemiology, prevention and management. Journal of Gastrointestinal Oncology. 2021; 12: S361–S373.

[4] Yang X, Li H, Liu J, Du C, He T, Luo X, *et al*. The short-term efficacy of DEB-TACE loaded with epirubicin and raltitrexed in the treatment of intermediate and advanced primary hepatocellular carcinoma. American Journal of Translational Research. 2021; 13: 9562–9569.

[5] Ma K, Liu J, Wang Y, Zhong Y, Wu Z, Fan R, *et al*. Relationship between plasma cell-free DNA (cfDNA) and prognosis of TACE for primary hepatocellular carcinoma. Journal of Gastrointestinal Oncology. 2020; 11: 1350–1363.

[6] Liang D, Yang B. Short-term efficacy of oral low-dose Tegafur chemotherapy after transarterial chemoembolization in primary hepatic carcinoma. Journal of B.U.ON. 2019; 24: 171–177.

[7] Chen M, Xu R, Wu L, Chen X. Relationship between circulating tumor cells undergoing EMT and short-term efficacy following interventional treatment in patients with hepatocellular carcinoma. Journal of Interventional Medicine. 2020; 3: 146–150.

[8] Bocci F, Zhou P, Nie Q. Single-Cell RNA-Seq Analysis Reveals the Acquisition of Cancer Stem Cell Traits and Increase of Cell-Cell Signaling during EMT Progression. Cancers. 2021; 13: 5726.

[9] Noronha C, Ribeiro AS, Taipa R, Castro DS, Reis J, Faria C, *et al*. Cadherin Expression and EMT: A Focus on Gliomas. Biomedicines. 2021; 9: 1328.

[10] Usman S, Waseem NH, Nguyen TKN, Mohsin S, Jamal A, Teh MT, *et al*. Vimentin Is at the Heart of Epithelial Mesenchymal Transition (EMT) Mediated Metastasis. Cancers. 2021; 13: 4985.

[11] Sompel K, Elango A, Smith AJ, Tennis MA. Cancer chemoprevention through Frizzled receptors and EMT. Discover. Oncology. 2021; 12: 32.

[12] Jones CA, Hazlehurst LA. Role of Calcium Homeostasis in Modulating EMT in Cancer. Biomedicines. 2021; 9: 1200.

[13] Brabletz S, Schuhwerk H, Brabletz T, Stemmler MP. Dynamic EMT: a multi-tool for tumor progression. The EMBO Journal. 2021; 40: e108647.

[14] Jiang Z, Zhang Y, Zhu Y, Li C, Zhou L, Li X, *et al*. Cathelicidin induces epithelial-mesenchymal transition to promote airway remodeling in smoking-related chronic obstructive pulmonary disease. Annals of Translational Medicine. 2021; 9: 223.

[15] Zhao X, Kong J, Zhao Y, Wang X, Bu P, Zhang C, *et al*. Gene

silencing of TACE enhances plaque stability and improves vascular remodeling in a rabbit model of atherosclerosis. Scientific Reports. 2015; 5: 17939.

[16] Zhang J, Chang Y, Xia H, Xu L, Wei X. HIST1H2BN induced cell proliferation and EMT phenotype in prostate cancer via NF-κB signal pathway. Genes & Genomics. 2021; 43: 1361–1369.

[17] Meng JF, Luo MJ, Li HB. Correlation between Plasma Cellular Retinoic Acid-Binding Protein 2 and Proliferation, Migration, and Invasion of Non-Small-Cell Lung Cancer Cells. Critical Reviews in Eukaryotic Gene Expression. 2021; 31: 81–89.

[18] Cheng M, Ye X, Dai J, Sun F. SOS1 promotes epithelial-mesenchymal transition of Epithelial Ovarian Cancer(EOC) cells through AKT independent NF-κB signaling pathway. Translational Oncology. 2021; 14: 101160.

[19] Morse B, Jeong D, Ihnat G, Silva AC. Pearls and pitfalls of response evaluation criteria in solid tumors (RECIST) v1.1 non-target lesion assessment. Abdominal Radiology (New York). 2019; 44: 766–774.

[20] Couchman JR. Syndecan-1 (CD138), Carcinomas and EMT. International Journal of Molecular Sciences. 2021; 22: 4227.

[21] Kumari N, Reabroi S, North BJ. Unraveling the Molecular Nexus between GPCRs, ERS, and EMT. Mediators of Inflammation. 2021; 2021: 6655417.

[22] Sisto M, Ribatti D, Lisi S. Organ Fibrosis and Autoimmunity: The Role of Inflammation in TGFβ-Dependent EMT. Biomolecules. 2021; 11: 310.

[23] Hu Y, Nie Q, Dai M, Chen F, Wu H. Histone Deacetylases Inhibit the Snail2-Mediated EMT During Metastasis of Hepatocellular Carcinoma Cells. Frontiers in Cell and Developmental Biology. 2020; 8: 752.

[24] Bhutia YD, Ogura J, Grippo PJ, Torres C, Sato T, Wachtel M, *et al*. Chronic exposure to excess iron promotes EMT and cancer via p53 loss in pancreatic cancer. Asian Journal of Pharmaceutical Sciences. 2020; 15: 237–251.

[25] Shin MR, Lee JA, Kim M, Lee S, Oh M, Moon J, *et al*. Gardeniae Fructus Attenuates Thioacetamide-Induced Liver Fibrosis in Mice via Both AMPK/SIRT1/NF-κB Pathway and Nrf2 Signaling. Antioxidants. 2021; 10: 1837.

[26] Liu Z, Sun J, Li C, Xu L, Liu J. MKL1 regulates hepatocellular carcinoma cell proliferation, migration and apoptosis via the COMPASS complex and NF-κB signaling. BMC Cancer. 2021; 21: 1184.

[27] Zhang Y, Ni W, Qin L. RUFY3 promotes the progression of hepatocellular carcinoma through activating NF-κB-mediated epithelial-mesenchymal transition. Aging. 2021; 13: 21283–21293.

[28] Shi J, Song S, Li S, Zhang K, Lan Y, Li Y. TNF-α/NF-κB signaling epigenetically represses PSD4 transcription to promote alcohol-related hepatocellular carcinoma progression. Cancer Medicine. 2021; 10: 3346–3357.

[29] Liu J, Wu Z, Han D, Wei C, Liang Y, Jiang T, *et al*. Mesencephalic Astrocyte-Derived Neurotrophic Factor Inhibits Liver Cancer Through Small Ubiquitin-Related Modifier (SUMO)ylation-Related Suppression of NF-κB/Snail Signaling Pathway and Epithelial-Mesenchymal Transition. Hepatology. 2020; 71: 1262–1278.

[30] Chen Y, Chen X, Ding X, Wang Y. Afatinib, an EGFR inhibitor, decreases EMT and tumorigenesis of Huh 7 cells by regulating the ERK VEGF/MMP9 signaling pathway. Molecular Medicine Reports. 2019; 20: 3317–3325.

[31] Yang H, Liang J, Zhou J, Mi J, Ma K, Fan Y, *et al*. Knockdown of RHOC by shRNA suppresses invasion and migration of cholangiocellular carcinoma cells via inhibition of MMP2, MMP3, MMP9 and epithelial-mesenchymal transition. Molecular Medicine Reports. 2016; 13: 5255–5261.

[32] Sun SJ, Wang N, Sun ZW, Chen J, Cui HW. MiR-5692a promotes the invasion and metastasis of hepatocellular carcinoma via MMP9. European Review for Medical and Pharmacological Sciences. 2018; 22: 4869–4878.

[33] Zhang H, Wang Z, Zhang Z. Hsa_circ_0009128 mediates progression of oral squamous cell carcinoma by influencing MMP9. Oral Diseases. 2023; 29: 661–671.

[34] Xu M, Zhang F, Wang A, Wang C, Cao Y, Zhang M, *et al*. Tumor Necrosis Factor-Like Weak Inducer of Apoptosis Promotes Hepatic Stellate Cells Migration via Canonical NF-κB/MMP9 Pathway. PLoS ONE. 2016; 11: e0167658.

[35] Zhao G, Wu H, Jiang K, Chen X, Wang X, Qiu C, *et al*. The Anti-Inflammatory Effects of Interferon Tau by Suppressing NF-κB/MMP9 in Macrophages Stimulated with Staphylococcus aureus. Journal of Interferon & Cytokine Research. 2016; 36: 516–524.

[36] Lv Y, Liu W, Ruan Z, Xu Z, Fu L. Myosin IIA Regulated Tight Junction in Oxygen Glucose-Deprived Brain Endothelial Cells Via Activation of TLR4/PI3K/Akt/JNK1/2/14-3-3ε/NF-κB/MMP9 Signal Transduction Pathway. Cellular and Molecular Neurobiology. 2019; 39: 301–319.